e-PS, 2006, **3**, 41-50
ISSN: 1581-9280 web edition
ISSN: 1854-3928 print edition

www.Morana-rtd.com

e-PRESERVATIONScience
published by MORANA RTD d.o.o.

IMAGING TOF-SIMS AND NANOSIMS STUDIES OF BARITE-CELESTITE PARTICLES IN GROUNDS FROM PAINTINGS BY VAN GOGH

FULL PAPER

B. MARINO[1], J. J. BOON[1 *], E. HENDRIKS[2], F. HORRÉARD[3], F. HILLION[3]

1. FOM-AMOLF, Kruislaan 407, 1098 SJ Amsterdam, The Netherlands
2. Van Gogh Museum, Paulus Potterstraat 7, 1071 CX Amsterdam, The Netherlands
3. CAMECA, 103, Boulevard Saint Denis, Courbevoie 92403, France

* corresponding author:
boon@amolf.nl

received: 06.11.2006
accepted: 19.12.2006

key words:
NanoSIMS, SIMS, Van Gogh, ground paint, barite, strontium

Abstract

In the late 19th century, Van Gogh like many painters would buy ready-made artists' materials. For matters of dating and authenticity, it is interesting to distinguish the different formulations and production batches, and to identify the nature and the source of the materials used. This information is useful also to point to different manufacturers, and is of relevance for studies of other impressionists besides Van Gogh.

One of the materials used as paint extender is barium sulphate. In its natural source, barite, barium can be replaced by strontium in a continuous solid solution series from barite ($BaSO_4$) to celestite ($SrSO_4$). In the process of making artificial barium sulphate most of the impurities are eliminated. Therefore, strontium can be used as an indication of natural barium sulphate in paints, and is potentially an interesting feature for discriminating different sources of the natural mineral.

Time-of-Flight Secondary Ion Mass Spectrometry (TOF-SIMS) and NanoSIMS are surface sensitive instruments that combine mass-spectrometric analysis with spatial resolution to give information on both the inorganic and organic fractions of a sample. In this paper we show their efficacy in the characterisation of the ground paint and in particular of barite-celestite in a painting by Van Gogh, *Plaster Figure of a Female Torso* (F216j, dated mid. June 1886).

1. Introduction

Time-of-Flight Secondary Ion Mass Spectrometry (TOF-SIMS) is a powerful technique that allows the investigation of both the inorganic and the organic fractions in a sample, and simultaneously combines high spatial and mass resolution. TOF-SIMS has been used in a variety of applications in surface analysis of materials such as polymers and semiconductors.[1] SIMS also proved extremely useful and efficient in the examination of the layer structure of paintings in paint cross-sections.[2] Its mapping capabilities allow the investigation of the nature and the distribution of paint materials within individual paint

layers, with a lateral resolution that is approximately 1 µm, depending on the image size. The advantage of SIMS over other imaging analytical techniques, such as SEM-EDX and imaging FTIR, is that it can analyse both the inorganic and organic components of the paint, providing information on the nature of both the pigment and the binding medium. An important benefit of static SIMS in probing the upper atomic layers of the surface is that no structural damage is visible. As paint cross-sections are single exemplars and are only available in limited supply, the advantages mentioned above make SIMS particularly useful for their study.

A new generation of ion microprobes is the CAMECA NanoSIMS 50, whose design ensures higher sensitivity combined with higher lateral and mass resolution.[3,4] This technique finds various applications in biology[5], material science[6], geochemistry and paleoceanography[7]. The high sensitivity and mass resolution also allow precise isotopic ratio measurement[8]. Ferreira et al.[9] used NanoSIMS in a multi-technique chemical microscopic study of the ground and preparatory layers in a paint cross-section from *Descent from the Cross*, a 15th-century painting by Rogier van der Weyden.

In this paper we explore and compare the capabilities of TOF-SIMS and NanoSIMS in the analysis of paint materials in a cross-section taken from a painting of Van Gogh's Paris period *Plaster Figure of a Female Torso* (F216j, dated mid. June 1886). Apart from a general survey, special attention will be given to barium sulphate ($BaSO_4$). Barium sulphate is used as extender in paints to reduce the production costs, as well as to improve the handling properties of the paint. Natural barium sulphate is preferred as an extender in cheaper paint preparations such as ground paints.[10] In the natural source of barium sulphate, barite, barium can be replaced by strontium in a continuous solid solution series from barite to celestite ($SrSO_4$).[11] In the process of making artificial barium sulphate a very pure product is obtained and most of the impurities are eliminated[12]. Therefore, strontium can be used as an indicator of natural barium sulphate in paints. In addition, it is potentially an interesting feature for discriminating between different sources of the natural mineral.[13] Like many other natural crystals, barite-celestite exhibits compositional oscillatory zoning, which consists of a more or less regular alternation of barium- and strontium-rich layers.[14] Studies on barites and barite-celestite solid solutions ($(Ba,Sr)SO_4$-H_2O) indicate that a correlation exists between the structural and physico-chemical characteristics of barite and its depositional environment.[15-18] The improved feature discrimination by NanoSIMS should allow an investigation of the distribution of barium and strontium in barite particles, and the characterization of their finer structural and substructural details.

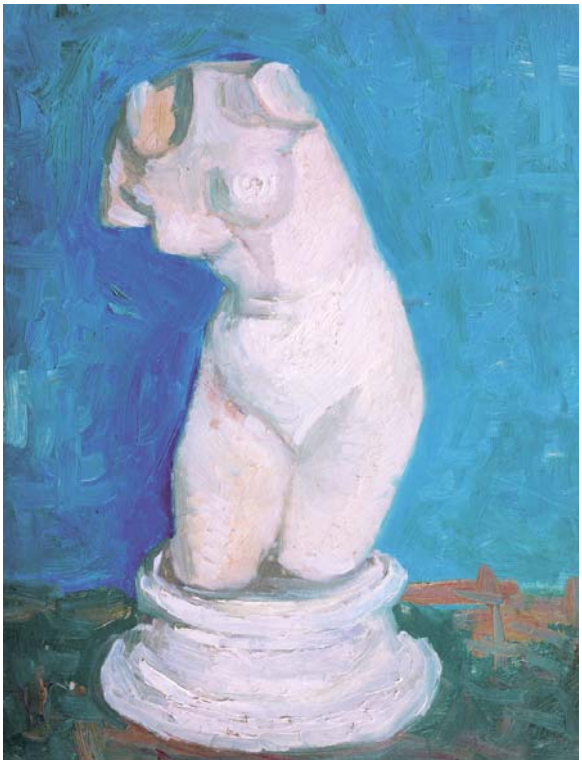

Figure 1: *Plaster Figure of a Female Torso* (F216j, mid. June 1886; Van Gogh Museum, Vincent van Gogh Foundation, Amsterdam).

2. Materials

2.1 Sample

The painting is made on cardboard, *carton* in French sources, pre-primed with a pale-grey ground of smooth (*à lisse*) surface texture. A picture of the painting is represented in Figure 1. An original trade sticker surviving on the back of the *carton* informs us that the support was purchased from the shop of Pignel-Dupont, established at the number 17 rue Lepic in Paris, just down the street from the apartment of Vincent's brother, where Vincent moved in June 1886. The sample was taken from along the bottom edge of the painting, where paper tape has been removed. The sample was embedded in polyester resin and polished with Micromesh paper to expose the paint at the surface and to achieve a flat surface.

2.2 Analytical techniques

2.2.1 Light Microscopy

Light microscopic images of the paint cross-section were acquired with a Nikon DX1200 24-bit colour digital still camera (Nikon Instech Co., Ldt., Japan) mounted on a Leica DMRX microscope (Leica, Wetzlar, Germany). Images were obtained under illumination provided by a 100 W tungsten-halogen lamp in visible light, and by an Osram

HBO 50W lamp and a Leica filter D (excitation 360-420 nm, emission > 460 nm) in UV light. Images under visible light were acquired in reflection mode in dark field.

2.2.2 TOF-SIMS

The static SIMS experiments were performed on a Physical Electronics (Eden Prairie, MN) TRIFT-II TOF-SIMS. Before acquisition with SIMS, the paint cross-section was carefully polished with increasing grades of Micromesh paper (up to 12000 grade), in order to avoid peak broadening in the mass spectra due to height differences of the sample surface, and to reduce effects of surface morphology on the ion yields. The sample surface was scanned with a 15 keV primary ion beam from an In^{115} liquid metal ion tip. The pulsed beam was non-bunched with a pulse width of 20 ns, a current of 600 pA and a spot size of ~120 nm. The primary ion beam was rastered over a 100 μm x 100 μm area, and the secondary ion signal was collected in an array of 256 x 256 points, each point collecting a full mass spectrum. Measurements were made both in positive and negative mode. In order to prevent charge accumulation on the insulating surface of the sample, the sample surface was charge compensated by means of an electron beam pulsed in between the primary ion beam pulses. To prevent large variations in the extraction field over the sample surface, a non-magnetic stainless-steel plate with a 1 mm-thick slit was placed on top of the sample. The paint cross-section was rinsed in hexane to reduce contaminations of polydimethylsiloxanes.

TOF-SIMS data were obtained under conditions of a sliding scale of mass resolutions ($m/\Delta M$ from 600 to 1500 over a mass range from 12 to 2000). The spectra are represented as nominal mass plots. Mass spectra were visualized at smaller mass ranges around elements or fragments of interest. Corresponding mass peaks were then carefully manually selected, also in order to minimize overlapping with organic fragments in positive spectra, and the resulting distribution maps plotted as images. Distribution maps aid in the identification of the materials present in the sample, and are most valuable when this is achieved through the comparison of multiple SIMS maps, and with a light-microscopic image of the analysed area, or with images obtained by means of other techniques.

After TOF-SIMS analysis the sample was gold-coated and examined with NanoSIMS.

2.2.3 NanoSIMS

Dynamic NanoSIMS measurements were performed with a CAMECA NanoSIMS 50. The CAMECA NanoSIMS 50 is a double focusing mass spectrometer that allows simultaneous collection of multiple masses by a system of five parallel detectors (or seven with the NS50L). The coaxial objective and extraction lens permit a very short working distance. This ensures low aberration coefficients for a high lateral resolution, and a quasi-full collection of the secondary ions, requisite for high transmission. All measurements are done at high mass resolution (without any slit or aperture in the spectrometer, $M/\Delta M$ = 2500). The NanoSIMS 50 is designed to work in dynamic SIMS mode. In contrast to TOF systems, its parallel detection mode allows continuous sputtering and therefore considerably higher secondary ion yields and shorter acquisition times.

The instrument is equipped with two reactive ion sources. Cs^+ primary ions are employed to detect negative secondary ions (ultimate resolution better than 50 nm). O^- primary ions are used to detect positive secondary ions (ultimate resolution better than 200 nm). Beam size, beam current, and number of pixels were chosen to optimise lateral resolution and acquisition time. The Cs^+ primary ion beam was operated at 16 keV, 6.4 or 2.8 pA current, and 150 or 100 nm spot size, and the O^- primary ion beam at 16 keV, 34, 13.9, 14.3, or 14.7 pA current, and 500 or 300 nm spot size. The images were acquired as 256 x 256 pixel images at scales varying between 25 and 100 μm, with a resulting effective resolution of 400, 150 and 100 nm for negative secondary ions images, and of 500 and 300 nm for positive ion images. The sample was gold coated (30 nm). This was sufficient to avoid any charging so no electron charge compensation was needed.

Backscattered electron images of the cross-section were taken after NanoSIMS analysis.

2.2.4 SEM-BSE

Scanning electron microscopy (SEM) analysis was performed on a XL30 SFEG high-vacuum electron microscope (FEI, Eindhoven, The Netherlands) with EDX system (spot analysis and elemental mapping facilities) from EDAX (Tilburg, The Netherlands). Backscattered electron (BSE) images of the cross-section were taken at 20 kV acceleration voltage at 5 and 6 mm eucentric working distance and spot size of 3 that correspond to a beam diameter of 2.2 nm with current density of ~ 130 pA.

3. Case study

Results of technical investigations by SEM-EDX and microchemical analysis made on the sample under investigation in a previous work by Hendriks and Geldof[19] revealed that the ground paint consists of lead white, little barium sulphate, gypsum, and few particles of carbon black and earth pig-

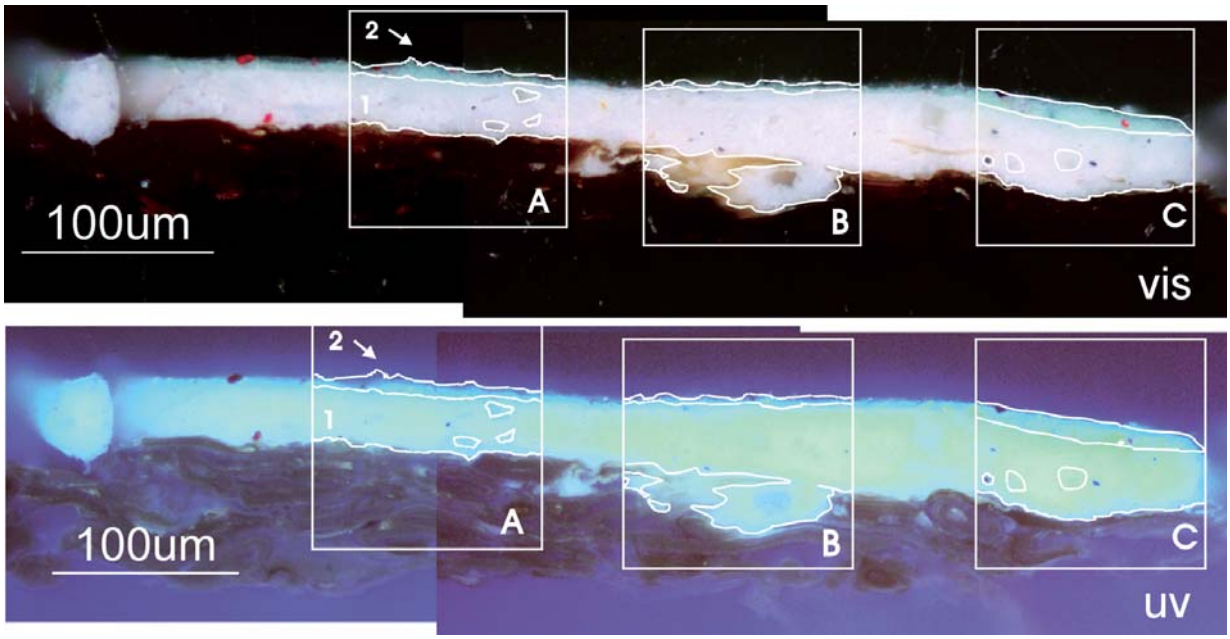

Figure 2: Paint cross-section F216j/1, light-microscopic images under visible (top) and UV light (bottom). The rectangular outlines in the light-microscopic images (A, B, C) indicate the areas mapped with TOF-SIMS.

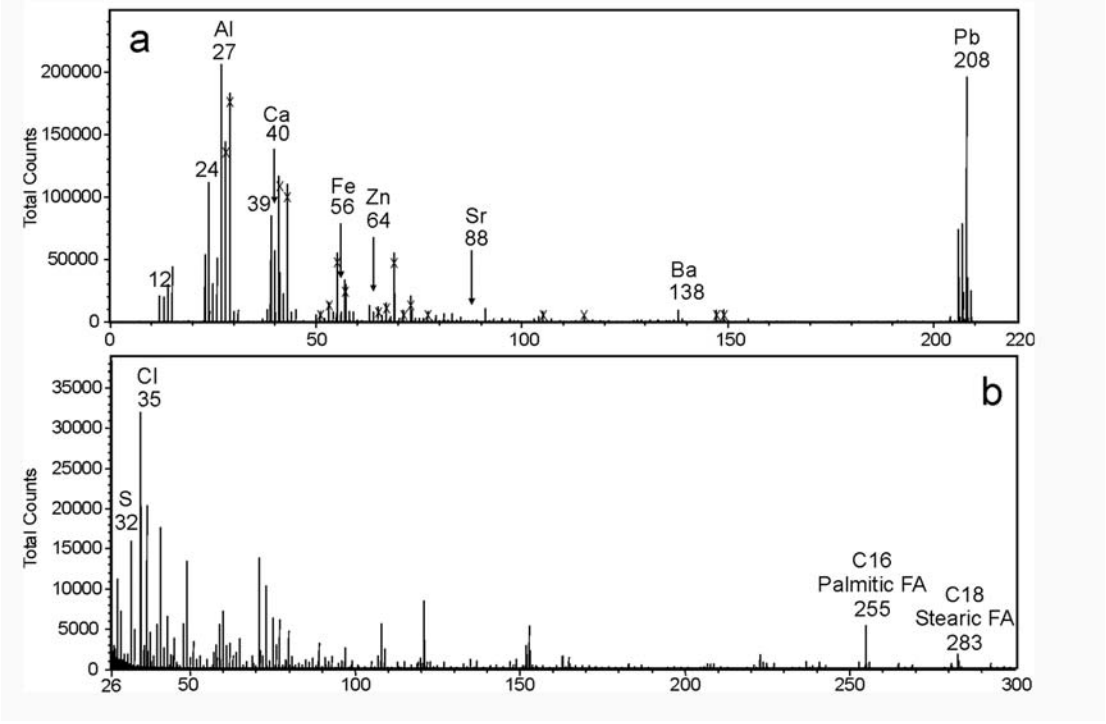

Figure 3: Example of TOF-SIMS spectra in positive (a) and negative (b) ion mode of the paint cross-section under investigation (X = polydimethyl siloxane, polyester, and phtalate contaminations; the peak at m/z 115 is produced by indium ions used to probe the sample surface).

ments. This composition is in agreement with the typical composition of commercial 19th-century ground paints.[10,20,21] This information was considered as a guide in the examination and interpretation of SIMS data.

3.1 Sample description and analysis by light microscopy

Light-microscopic images of the cross-section under visible and UV light are shown in Figure 2. The sample contains a thin light blue paint layer (layer 2, up to 10 µm thick), the ground layer (layer 1, 20-25 µm thick), and fibres from the support. The bluish paint contains also orange and red particles. The ground layer includes transparent particles and a few black, red and ochreous particles. Several blue-fluorescing spots appear in the light blue layer under UV light.

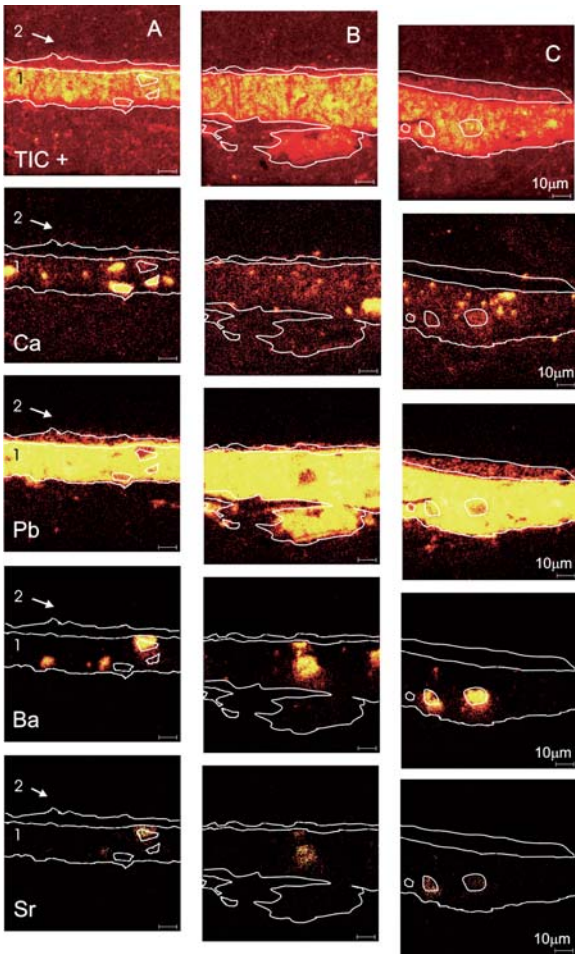

Figure 4: Paint cross-section F216j/1, TOF-SIMS total ion current image and distribution maps of characteristic elements in positive mode.

3.2 Spectral SIMS information

The paint cross-section has been analysed in three areas (indicated in the light-microscopic image with letters from A to C). Two TOF-SIMS spectra, acquired in both positive and negative ion mode and corresponding to the entire probed area, are shown in Figure 3. Characteristic mass peaks of the ground paint are those of lead (*m/z* 208), calcium (*m/z* 40), barium (*m/z* 138), strontium (*m/z* 88), iron (*m/z* 56), aluminium (*m/z* 27), and potassium (*m/z* 39) in positive mode, sulphur (*m/z* 32), chlorine (*m/z* 35), and deprotonated $[M - H]^-$ palmitic (*m/z* 255) and stearic (*m/z* 283) acids in negative mode. The blue paint layer is characterized by lead and zinc (*m/z* 64). The distribution maps (Figures 4-6) characterize the paints as follows.

3.2.1 Barite in the ground paint

Detection of barium (Figure 4) and sulphur (Figure 6) reveal the presence of barium sulphate ($BaSO_4$) in the ground paint layer (layer 1). Under the light microscope in visible light, barium sulphate in oil paint appears transparent, because of its similar refractive index.

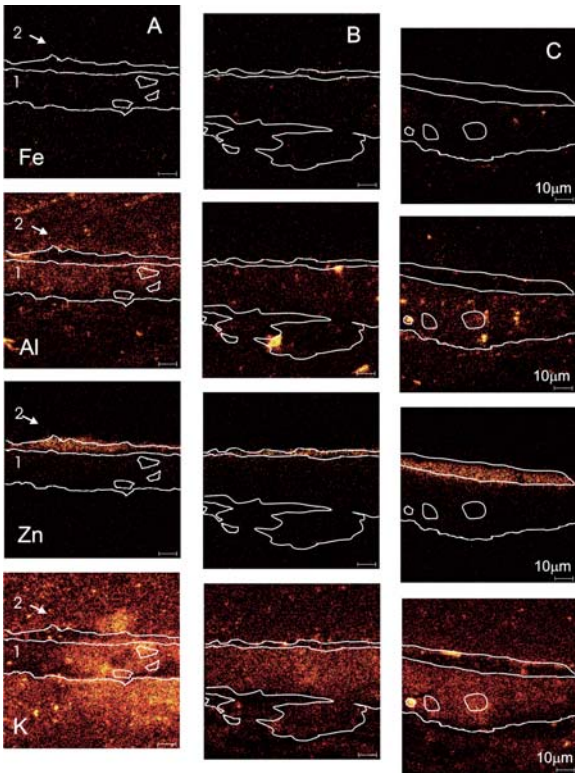

Figure 5: Paint cross-section F216j/1, TOF-SIMS distribution maps of characteristic elements in positive mode.

The clear co-occurrence of barium and strontium (Figure 4) is an indication of the natural origin of barium sulphate. In fact, the natural source of barium sulphate, barite, which is the most common barium mineral, is generally pure $BaSO_4$, however barium can be replaced by strontium in a continuous solid solution series from barites to celestite ($SrSO_4$). Barites of this series with a preponderance of barium are called strontiobarites.[11] We also observe in the distribution maps that the relative intensity distributions of these two elements vary over the different particles. In the process of making artificial barium sulphate a very pure product is obtained and most of the impurities are eliminated.[12] Therefore, strontium can be used as an indicator of natural barium sulphate in paints; in addition, it is potentially an interesting feature for discriminating between different sources of the natural mineral.[13]

3.2.2 Other materials in the ground paint

The distribution maps reveal that the ground paint consists of massive amounts of fine-grained lead white, mixed with particles of varying sizes of calcium carbonate and gypsum, and of barium sulphate, which was discussed above.

Lead white (leadhydroxycarbonate, $2PbCO_3 \cdot Pb(OH)_2$) is the main white component of the ground paint and can be identified from the map of lead. Chlorine is associated with lead (Figure 4) as chloride (Figure 6), as is evident from the very high

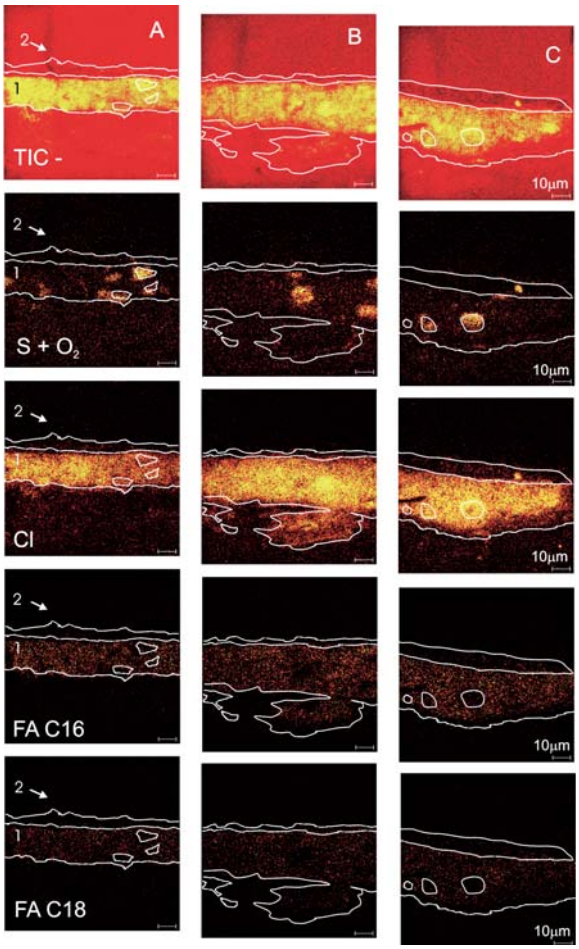

Figure 6: Paint cross-section F216j/1, TOF-SIMS total ion current image and distribution maps of characteristic elements in negative mode.

correlation between their distributions.[22] The source of chlorine and its form in the paint are unknown.

Calcium (Figure 4) is found in calcium carbonate ($CaCO_3$) and gypsum (calcium sulphate, $CaSO_4$), the co-occurrence of sulphur (Figure 6) with calcium being indicative of gypsum. Calcium carbonate as well as finely ground gypsum are commonly mixed with lead white as cheap adulterants in oil ground paint preparations.[10,23] Some spots in the maps of aluminium, silicon, potassium and iron (Figure 5; silicon not shown) are indicative of clay, silica, and iron oxides and hydroxides. The literature informs us that these materials are commonly included in the ground paint as extenders and impart a tint to the ground[23]. However, in recent work Marino[24] suggests that alternatively, cheaper, impure materials might have been used in the making of cheap grounds, and that the tint is imparted by the presence of impurities rather than by addition of separate materials. In fact, clay, silica and iron oxides could also point to a marl as a calcium carbonate source. Marls are very common forms of limestone in Tertiary rocks of the Paris Basin area, which is a likely source of the calcium carbonate used in the ground paint under study.[24]

The oil binding medium is characterized by the peaks of deprotonated $[M - H]^-$ palmitic (C16: *m/z* 255) and stearic acids (C18: *m/z* 283) in negative mode spectra. The relative amount of palmitic over stearic fatty acid (called P/S ratio) characterizes oils used as binding media as follows: P/S < 2 linseed oil, P/S > 2.5 walnut or poppy oil, P/S > 5 poppy oil,[25-27] assuming that oil mixtures were not used. The distributions of fatty acids (Figure 6) in the paint cross-sections closely resemble the distribution of lead (Figure 4). It has been already observed by Keune[25] that pseudo molecular ions from fatty acids have a relatively higher yield near the lead white particles, a fact suggesting assistance of lead in the secondary ion formation or higher relative concentration of fatty acids on the surface of lead white. The values of the P/S ratio in this case are inconclusive with respect to the type of oil used as the binding medium (respectively 2.4, 2.4, and 2.3 in areas A, B, and C).

3.2.3 Materials in the upper paint layer

The blue paint layer (layer 2) is characterized by the presence of lead white, in lower amounts than in the ground paint, and of zinc white (the source of the fluorescence), with no evidence in SIMS data of coloured materials. The maps of lead and zinc are depicted in Figure 4. Zinc white (zinc oxide, ZnO_2) was commonly used in tube-paint formulations as a lightening agent to adjust the colour in artists' paints.[20]

According to the earlier microchemical analysis, performed by treatment with 4M NaOH, the blue paint layer loses its colour, indicating that Prussian blue is the source of the blue colour.[28, 29] Prussian blue can be identified with SIMS through the characteristic negative ion clusters of ferrocyanide.[30] Unfortunately, static SIMS analysis on these samples did not give any evidence of either ferrocyanides in negative spectra, nor of iron in positive spectra. However, Prussian blue is a pigment of very deep blue colour, and is usually ground very finely and used mixed with white pigment (e.g. lead white or zinc white). It is therefore likely that, even if Prussian blue is present, the particle size of the pigment is so small and its concentration so low that they are well below the detection limit of the instrument.

A 'hot' spot in the map of sulphur (Figure 6) can be correlated to a red particle in the light-microscopic image, suggesting the presence of vermilion (mercuric sulphide, HgS). Mercury was not detected because of its poor ionisation with TOF-SIMS. Other red particles remain undetected; the presence of other types of red pigment can therefore not be excluded.

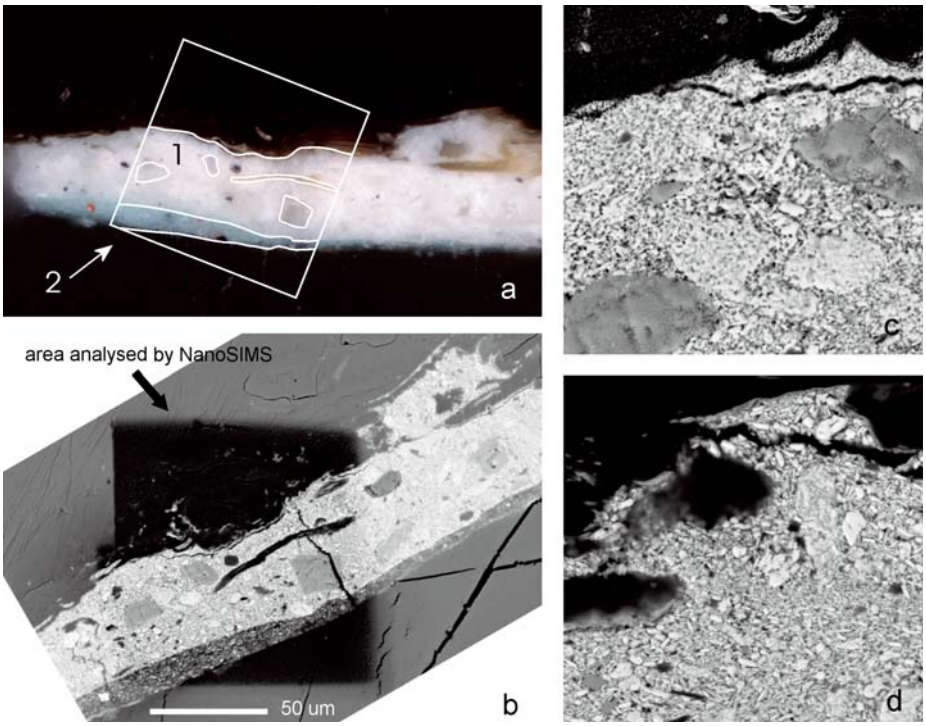

Figure 7: Light-microscopic (a) and SEM-BSE (b) images showing the area analysed by NanoSIMS. Two BSE images acquired at higher magnification (in two different areas) show the damage caused by the sputtering process (c) compared to the undamaged surface, exposed after repolishing of the paint cross-section (d). In these images the ground layer is on top to match the orientation of the NanoSIMS images.

Minute amounts of the same aluminium-containing materials found in the ground paints were found in the upper paint layer as well.

3.2.4 Texture analysis from SIMS maps

The maps of lead, calcium and barium, show that the ground layer (layer 1) has a very fine and homogeneous texture of mostly fine (sub)-micron particles and some larger particles (1-10 μm) of calcium carbonate, gypsum, barium sulphate and lead white. Barium sulphate particles lie in the size range up to 10-15 μm with preponderance of the larger ones. Lead white and zinc white give the blue upper paint (layer 2) a very fine and homogeneous texture in the (sub)-micron size range.

3.3 Interpretation of nanosims data

The mass information obtained by NanoSIMS is distinct from that obtained by static SIMS. The ion dosage and energy in each analysed spot are higher and only small fragments and elements can be detected by this method.

Distribution maps of carbon (*m/z* 12), oxygen (*m/z* 16), nitrogen (detected as CN^-, *m/z* 26), sulphur (*m/z* 32), chlorine (*m/z* 35) as negative secondary ions, and sodium (*m/z* 23), calcium (*m/z* 40), strontium (*m/z* 88), barium (*m/z* 138) as positive secondary ions were acquired. Chlorine was used instead of lead as a marker of lead white, to which it is associated. Because of the parallel positioning of the detectors, the choice of chlorine allowed the acquisition of element maps over a smaller mass range and consequently at higher mass resolution.

The area analysed by NanoSIMS is outlined in the light-microscopic image illustrated in Figure 7a. A SEM-BSE micrograph of the sample surface after sputtering off of the gold layer and NanoSIMS analysis is shown in Figure 7b. The exposed analysed area appears as a darker rectangular region. A close-up view of the region shows the damage caused by the sputtering process (Figure 7c). The BSE detection was set up in order to optimise atomic number contrast; because of differences in atomic numbers and therefore of backscattered electrons yields, lead, barium and calcium appear respectively in white, grey and black. The elemental distribution maps obtained by NanoSIMS are depicted in Figures 8-11. These maps allow the identification of paint materials as discussed in the previous section for TOF-SIMS analysis. In addition, in contrast with static SIMS, NanoSIMS provides better resolution, and a higher sensitivity due to the dynamic regime. As it will be illustrated later in the text, NanoSIMS also

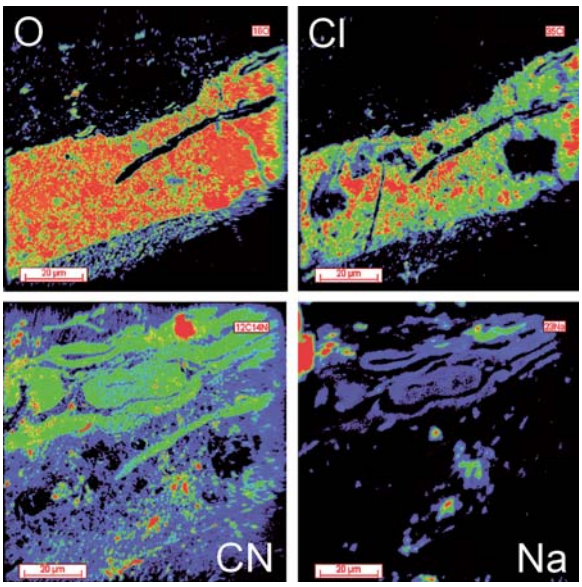

Figure 8: NanoSIMS maps of oxygen, chlorine, nitrogen (detected as CN^- where carbon is also present), and sodium.

allows to performing quantitative isotopic characterization.

Distribution maps of oxygen, chlorine, CN^-, and sodium are depicted in Figure 8. Oxygen is present in association with lead white, calcium carbonate, gypsum, barite, and with the binding medium. The chlorine map follows the distribution of lead white in the ground paint.

The cardboard fibres are clearly visible in the CN^- and sodium maps. The advantage of NanoSIMS compared to static SIMS is a better sensitivity to nitrogen detected in the form of CN^-, which is a reaction product of the sputtering process when both nitrogen and carbon are present in the analysed spots. The nitrogen component associated to the fibres can be indicative of protein residues in the plant cell walls, of an attempt to glue the fibres together in the manufacturing of the cardboard,[31] or of application of a water-based size prior to the ground. CN^- seems to be abundant also in the paint layers, most likely as ammonia or nitrate impurity in lead white (this fragment is also observed in lead white oil paint reconstructions when NanoSIMS is performed[32]).

Sodium is another feature, possibly naturally present in the fibres or introduced during the manufacturing process of the cardboard, or as residues of sodium hydroxide or sodium chlorate in the preparation the cardboard pulp. In the latter case, chlorine is not observed in the cardboard as it reacts away in the bleaching process.

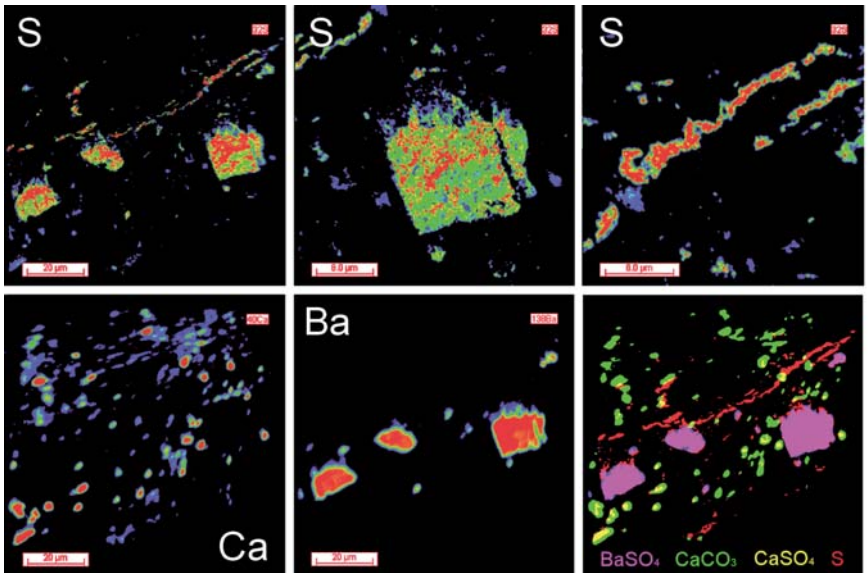

Figure 9: Images of sulphur indicate gypsum and barite particles (where there is co-occurrence with calcium and barium). The overlay of sulphur, barium and calcium represented in the bottom right corner represents particles of barite (in magenta), gypsum (in yellow) and calcium carbonate (in green). The thin line of sulphur along the contact zone of the ground paint layer with the cardboard appears in red.

The sulphur maps in Figure 9 show particles of barium sulphate (in combination with barium) and gypsum (in combination with calcium). The higher sensitivity of NanoSIMS compared to static SIMS to sulphur improves the discrimination between calcium carbonate and gypsum. The sulphur map also exhibits a thin line along the contact zone between the priming layer and the cardboard. The sulphur and chlorine maps show that sulphur and lead overlap along this line. It can be observed also in the SEM-BSE image that the line lies along the edge of the lead paint (appearing in white because of the high electron backscattering).

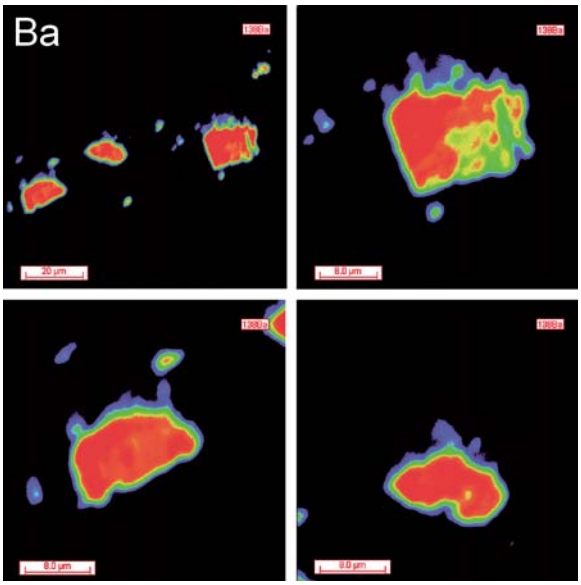

Figure 10: NanoSIMS distribution maps of barium, overview (top left) and at higher magnification for individual particles.

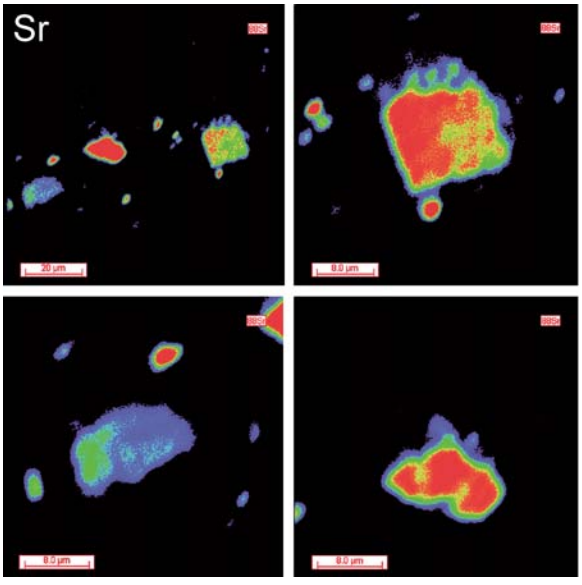

Figure 11: NanoSIMS distribution maps of strontium, overview (top left) and at higher magnification for individual particles.

Sulphur might have been absorbed as sulphide or sulphur oxide by the cardboard from the atmosphere before application of the ground paint, and could have reacted subsequently with lead white to form lead sulphate.

In the bottom right of Figure 9 an overlay of the maps of sulphur, calcium and barium shows the distribution of calcium carbonate, gypsum, barium sulphate, and the thin line of sulphur.

Compared to static SIMS, NanoSIMS shows better sensitivity also to strontium. Combined with its high resolution, it was possible to characterize finer structural and sub-structural details of barite particles and to measure differences in relative concentrations. Specifically, barium and strontium show uneven distributions, with between- and within-particle differences in relative concentrations (Figures 10-11). Barite-celestite ($(Ba,Sr)SO_4$-H_2O) solid solutions exhibit a relationship between crystal size, morphology and composition[20]. The (uncalibrated) ion yields ratio of strontium to barium, measured at different spots in two particles, fluctuates between 0.7% and 3% in one particle and between 0.4% and 0.61% in the other. Although not observed here, the oscillatory zoning characteristic of barite-celestite does not make the relative concentration of strontium-to-barium useful for tracing the different sources of the mineral.

Instead, the $^{86}Sr/^{87}Sr$ isotope ratio seems to be a more promising tool for this purpose. Strontium and sulphur isotope ratios are considered useful tools for distinguishing between barites of different origins and ages.[15, 16] In the field of authentication and origin assignment, isotopic characterization has already been successfully tested for lead in lead white paints.[33] The capability of NanoSIMS for isotopic characterization of barite was also tested by measuring the strontium $^{86}Sr/^{87}Sr$ isotope ratio in one particle. The obtained value of 0.718 falls within the range considered characteristic of non-marine barites as indicated for example by Castorina et al.[15] Paytan et al.[17] suggest to combine strontium and sulphur isotopic analyses with a crystal-morphology characterization to provide a reliable indicator of the depositional environment of a given barite.

4. Conclusions

With static SIMS we were able to investigate the material composition and the textural characteristics of the paint layers in painting cross-sections. TOF-SIMS allowed analysis of both the pigment and the binding medium content, providing information on their spatial distribution. Although the analysis was mainly focused on the ground paint layer, it is expected that the technique will be successfully applicable also to the paint layer. The combination of these characteristics enables us to identify and differentiate the different materials in the paint layers, and at the same time to examine the texture of the particulate materials individually.

In the painting under investigation we were able to detect and identify all the major components of the ground paints, lead white, calcium carbonate, gypsum, and barium sulphate. Barium sulphate is in its natural form, as it was found in association with strontium. TOF-SIMS data also show different grades of coarseness for the paint. For elements of higher detection efficiency, yields reflected the morphology of individual particles, provided that these are sufficiently large compared to the instrumental lateral resolution at the analytical conditions used.

The results of the explorative investigation presented in this paper shows the potential of NanoSIMS for the analysis of paint cross-sections. Compared to TOF-SIMS, NanoSIMS exhibits higher sensitivity and a higher lateral and mass resolution, both of which can be achieved simultaneously. In the case study considered, the improved features provided additional information that could not be obtained by TOF-SIMS. These include the enhanced detection of fine sub-structural details within barite particles and of other fine structures in the paint cross-section, of key trace elements and of organic markers. This work demonstrated that NanoSIMS can be used to measure differences in relative concentrations of strontium to barium, to examine the distribution of barium and strontium within and between barite particles, and to perform isotope analysis of strontium in barites. Strontium and sulphur isotopic ratios seem promising tools for to distinct different sources of barite used in paints. More extensive work on barite in paints involving the development/consultation of a database of barites from different locations is required. The analytical potential presented by NanoSIMS for the characterization of barites shows that this technique can assist in the distinction of different sources of the barite in paints.

Acknowledgements

The samples were provided by Ella Hendriks (Van Gogh Museum, Amsterdam). We thank Stefan Luxembourg and Liam McDonnell (AMOLF, Amsterdam) for technical assistance with SIMS instrumentation, and Katrien Keune (AMOLF) for assistance in the acquisition and interpretation of SIMS data specifically for paint cross-section samples. François Hillion and François Horreard (Cameca, Courbevoie, France) are gratefully acknowledged for providing the NanoSIMS facilities and for the processing of the data. Muriel Geldof (ICN, Amsterdam) is thanked for providing information on earlier investigations made on the sample.

References

1. J.C. Vickerman et al., *ToF-SIMS: Surface Analysis by Mass Spectrometry*, J.C. Vickerman, D. Briggs (Eds.), IM Publication and Surface Spectra Limited, West Sussex and Manchester, 2001, **18-28**, 497-778.

2. K. Keune, E. Ferreira, J.J. Boon, *Characterization and localisation of the oil binding medium in paint cross-sections using imaging secondary ion mass spectrometry*, Proceedings of the 14th Triennial Meeting of the ICOM Committee for Conservation in the Hague, The Netherlands, September 12-16, 2005, 796-802.

3. M. Schuhmacher, F. Hillion, *Ultra fine feature analysis using secondary ion emission*, Proceedings 2nd NIRIM International Symposium on Advanced Materials (ISAM 95), 1995. http://www.cameca.fr/html/publications.html, accessed 18.12.2006

4. M. Schuhmacher, B. Rasser, E. De Chambost, F. Hillion, Th. Mootz, H.-N. Migeon, *Recent instrumental developments in magnetic sector SIMS*, Fresenius Journal of Analytical Chemistry, 1999, **365**, 12-18.

5. N. Grignon, J.J. Vidmar, F. Hillion, B. Jaillard, *Physiological application of the NanoSIMS 50 ion microscope: localization at subcellular level of ^{15}N labelling in Arabidopsis Thaliana*, Proceedings of the 12th International Conference of Mass Spectrometry, Brussels, Belgium, 5-11 September 1999, 903-906.

6. P. Bou, L. Vandenbulcke, R. Herbin, F. and Hillion, *Diamond film nucleation and interface characterization*, Journal of Materials Research, 1992, **7,** 2151-2159.

7. A. Meibom, J.P. Cuif, F. Hillion, B.R. Constantz, A.J. Leclerc, Y. Dauphin, T. Watanabe, R.B. Dunbar, *Distribution of magnesium in coral skeleton*, Geophysical Research Letters, 2004 , **31**, L23306.

8. R.A. Stern, I.R. Fletcher, B. Rasmussen, N.J. McNaughton, B.J. Griffin, *Ion microprobe (NanoSIMS 50) Pb-isotope geochronology at < 5 μm scale*, International Journal of Mass Spectrometry, 2005, **244**, 125-134.

9. E.S.B. Ferreira, K. Keune, J.J. Boon, *Combined microscopic analytical techniques as diagnostic tools in the study of paint cross-sections: case study of a sample from a 15th century painting, The Descent from the Cross by Rogier van der Weiden*, Proceedings of the 4th Biennial Meeting of the IPCR (Instituto Portugues de Concervação e Restauro), 2005.

10. L. Carlyle, *The artist's assistant: oil painting instruction manuals and handbooks in Britain 1800-1900 with reference to selected eighteenth century sources*, Archetype Publications, London, 2001.

11. W.A. Deer, R.A. Howie, J. Zussman, *An introduction to the rock-forming Minerals,* Longmans, London, 1967, 462-464.

12. R. Feller, *Barium sulphate - natural and synthetic*, in: *Artists' pigments: a handbook of their history and characteristics*, National Gallery of Art, Washington, 1986, 47-64.

13. B. Marino, K. Keune, E. Hendriks, J.J. Boon, *SIMS studies of the material aspects in grounds and paints in paintings by Van Gogh*, Conference Proceedings Art'05: 8th International Conference on Non-destructive Testing and Microanalysis for the Diagnostics and Conservation of the Cultural and Environmental Heritage, Lecce, Italy, 15-19 May, 2005.

14. I. L'Heureux, S. Katsev, *Oscillatory zoning in a (Ba,Sr)SO_4 solid solution: macroscopic and cellular automata models*, Chemical Geology, 2006, **225**, 230-243.

15. J.-G. Bréhéret, H.-J. Brumsack, *Barite concretions as evidence of pauses in sedimentation in the Marnes Bleues formation of the Vocontian Basin (SE France)*, Sedimentary Geology, 2000, **130**, 205-228.

16. F. Castorina, E. di Biasio, U. Masi, L. Tolomeo, *Strontium isotope evidence for the origin of barite from four mineralizations of the Moroccan Meseta*, Journal of African Earth Sciences, 1999, **29**, 619-625.

17. A. Paytan, S. Mearon, K. Cobb, M. Kastner, *Origin of marine barite deposits: Sr and S isotope characterization*, Geology, 2002, **30**, 747-750.

18. N. Sánchez-Pastor, C.M. Pina, L. Fernández-Díaz, *Relationships between crystal morphology and composition in the (Ba,Sr)SO_4-H_2O solid solution-aqueous solution system*. Chemical Geology, 2006, **225**, 266-277.

19. E. Hendriks, M. Geldof, *Van Gogh's Antwerp and Paris picture supports (1885-1888) reconstructing choices*, ArtMatters Netherlands Technical Studies in Art, 2005, **2**, 39-74.

20. D. Bomford, J. Leighton, J. Kirby, A. Roy, *Art in the making: Impressionism*, National Gallery London Publications, Yale University Press, New Haven and London, 1991.

21. A. Callen, *The art of Impressionism: painting technique & the making of modernity*, Yale University Press, New Haven and London, 2000.

22. K. Keune and J.J. Boon, *Imaging Secondary Ion Mass Spectrometry of a paint cross-section taken from an Early Netherlandish painting by Rogier van der Weyden*, Analytical Chemistry, 2004, **76**, 1374-1385.

23. R.J. Gettens, G.L. Stout, *Painting materials - A short encyclopaedia*, Dover Publications Inc., New York, 1966.

24. B. Marino, *Paints quantified: Image analytical studies of preparatory grounds used by Van Gogh*, Ph.D. Thesis, University of Amsterdam, 2006.

http://www.amolf.nl/publications/theses/, accessed 18.12.2006.

25. K. Keune, *Binding medium, pigments and metal soaps characterised and localised in paint cross-sections*, Ph.D. Thesis, University of Amsterdam, 2005.

http://www.amolf.nl/publications/theses/, accessed 18.12.2006.

26. M.R. Schilling, H.P. Khaijan, *Gas chromatographic determination of fatty acid and glycol content of lipids I. The effect of pigments and aging on the composition of oil paints*, Preprints of the 11th triennial meeting of the ICOM Committee for Conservation, Edinburgh, United Kingdom, 1996, **1**, 242-247.

27. J.S. Mills and R. White, *The organic chemistry of museum objects*, Butterworth 1987.

28. B.H. Berrie, *Prussian Blue*, in *Artists' pigments: A handbook of their history and characteristics*, vol. 1, Robert L. Feller (Ed.), National Gallery of Art, Washington, D.C., 1986.

29. J.Plesters, *Cross-sections and chemical analysis of paint samples*, Studies in Conservation, 1955/56, **2**, 110-157.

30. K.J. Van der Berg, R. Heeren, *Secondary Ion Mass Spectrometry on paint cross-sections*, Molart report 1995-98*,* 1998, 83.

31. P. Bower, *A brush with nature: an historical and technical analysis of the papers and boards used as supports for landscape oil sketching*, in: Works of Art on Paper: Books, Documents and Photographs, International Institute of Conservation (ICC) Contributions to the Baltimore Congress 2002, 16-20.

32. Unpublished test results.

33. G. Fortunato, A. Ritter, D. Fabian, Old Masters' lead white pigments: investigations of paintings from the 16th to the 17th century using high precision lead isotope abundance ratios, The Analyst, 2005, **130**, 898-906.